



Cite this: *Chem. Commun.*, 2017, 53, 4358

Received 2nd March 2017,  
Accepted 24th March 2017

DOI: 10.1039/c7cc01628j

rsc.li/chemcomm

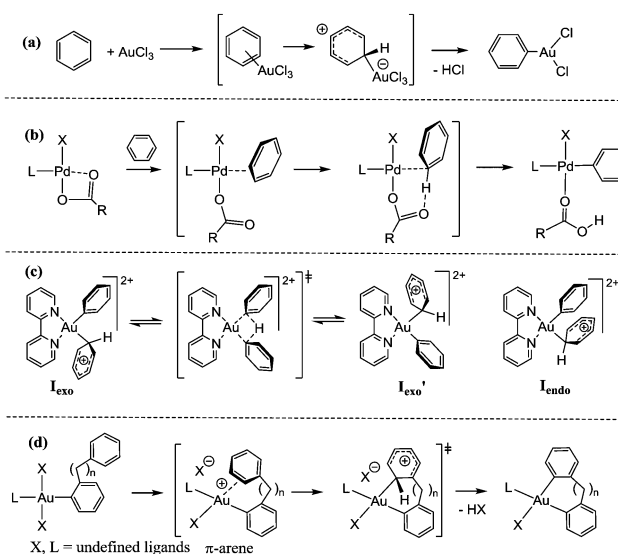
# Arene C–H activation by gold(III): solvent-enabled proton shuttling, and observation of a pre-metallation Au–arene intermediate†

L. Rocchigiani,<sup>a</sup> J. Fernandez-Cestau,<sup>a</sup> P. H. M. Budzelaar\*<sup>b</sup> and M. Bochmann <sup>a</sup>

**Selective Au–C bond cleavage and arene–C–H activation in (C<sup>^</sup>N<sup>^</sup>C)Au(III) pincer complexes are reversible, leading to a solvent-dependent proton shuttling process. The ether-free cleavage products are non-fluxional and show weak gold(III)–arene interactions commensurate with intermediates postulated for CMD-type arene activation.**

The metallation of arene C–H bonds is an important synthetic tool. Since these reactions are frequently highly site-selective, they have become a method of choice for C–C bond formations and arene functionalizations.<sup>1</sup> Compared to other noble metals, the C–H activation by gold and formation of cyclometallated gold aryl complexes is synthetically more limited and often very sensitive to the nature of arene substituents. This notwithstanding, cyclometallations form the basis of several types of gold pincer complexes<sup>2,3</sup> which find widespread use ranging from photoluminescent compounds<sup>4,5</sup> to anti-cancer agents.<sup>6</sup>

The activation of aromatic C–H bonds by gold trichloride to give arylgold halide complexes was first reported in the 1930s.<sup>7</sup> The reaction most probably proceeds by an S<sub>E</sub>Ar pathway and involves attack of an electrophilic metal ion on the arene π-system, followed by HCl elimination. This mechanism is characterized by a zwitterionic Wheland intermediate in which there is significant distortion of the C–H bond angle (Scheme 1a). Since it proceeds *via* a cationic intermediate, this path is favoured by electron donating ring substituents.<sup>8</sup> On the other hand, basic gold complexes react smoothly with fluorinated arenes to give the corresponding gold aryl products.<sup>9,10</sup> For reactions of this type, an alternative mechanism is favoured: Concerted Metallation-Deprotonation (CMD). This pathway is well established for arylations and cyclometallations of palladium,<sup>11</sup> and is characterized by only small angular distortion of the arene C–H bond and weak π-interaction between the metal and the arene ring



**Scheme 1** (a) Arene auration by AuCl<sub>3</sub> *via* the S<sub>E</sub>Ar mechanism;<sup>7</sup> (b) arene metallation by concerted metallation–deprotonation (CMD);<sup>11–13</sup> (c) hypothetical degenerate H-exchange in an Au<sup>III</sup>(phenyl)(benzene) model complex;<sup>14</sup> (d) proposed arene C–H activation pathway in Au<sup>III</sup>-catalysed arene–arylsilane coupling.<sup>15</sup>

(Scheme 1b). The metal–arene interaction needs to be just sufficiently strong to increase the acidity of the C–H bond to facilitate abstraction by a base, such as acetate. CMD reactions have been probed mechanistically and computationally and, in the case of metal acetates, involve a 6-membered cyclic intermediate. For palladium this mechanism has been demonstrated for a wide range of arenes and heteroarenes.<sup>12,13</sup>

To the best of our knowledge, for gold(III) there is only one report of a computational investigation of the arene metallation mechanism, on the solvent-free reversible activation of benzene by the [(bipy)AuPh]<sup>2+</sup> dication. In this case an energy minimum for an η<sup>2</sup>-benzene adduct could not be located, but Wheland-type η<sup>1</sup> intermediates are thought to be formed (Scheme 1c). A proton exchange pathway involving the two *ipso*-carbon atoms was found

<sup>a</sup> School of Chemistry, University of East Anglia, Norwich Research Park, Norwich, NR4 7TJ, UK. E-mail: m.bochmann@uea.ac.uk

<sup>b</sup> Department of Chemical Sciences, Federico II University of Naples, Via Cintia, 80126 Napoli, Italy. E-mail: p.budzelaar@unina.it

† Electronic supplementary information (ESI) available: Synthesis, NMR spectroscopic and computational details. See DOI: 10.1039/c7cc01628j



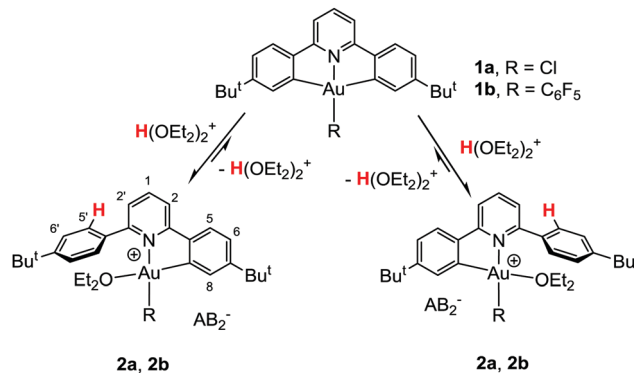
to be energetically slightly favoured, with a reaction barrier of  $7.8 \text{ kcal mol}^{-1}$  with reference to the *exo* intermediate  $\mathbf{I}_{exo}$ . However, no experimental evidence for benzene activation by  $[(\text{bipy})\text{AuPh}(\text{L})]^{2+}$  ( $\text{L} =$  weakly coordinating ligand) or  $[(\text{bipy})\text{AuPh}_2]^+$  could be found.<sup>14</sup> Similar processes have been invoked in catalytic and kinetic studies on gold(III) mediated intra- and intermolecular oxidative aryl-aryl coupling reactions of arylsilanes. The intramolecular version of this reaction proved particularly amenable to detailed kinetic investigations, and on the basis of Hammett relationships, an  $\text{S}_{\text{E}}\text{Ar}$ -type arene activation mechanism was preferred (Scheme 1d).<sup>15</sup>

Instructive as such kinetic studies are, the nature of intermediates and transition states must remain a matter of conjecture, and the ligand sphere of the gold species thought to be involved in catalysis remains ill-defined. We set out therefore to study the intramolecular activation of arenes in a well-defined system, based on the selective Au–C bond cleavage of  $(\text{C}^{\wedge}\text{N}^{\wedge}\text{C})\text{AuX}$  pincer complexes<sup>10</sup> with acid ( $\text{C}^{\wedge}\text{N}^{\wedge}\text{C} = 2,6\text{-}(\text{C}_6\text{H}_3\text{Bu}^t)_2\text{pyridine}$  dianion). We showed earlier that such pincer complexes react with trifluoroacetic acid under selective cleavage of one of the Au–C bonds to give the chelate  $(\text{C}^{\wedge}\text{N}\text{-CH})\text{Au}(\text{X})(\text{OAc}^{\text{F}})$ .<sup>16</sup> We report here the Au–C cleavage reaction of  $(\text{C}^{\wedge}\text{N}^{\wedge}\text{C})\text{AuX}$  ( $\mathbf{1a}$ ,  $\text{X} = \text{Cl}$ ;  $\mathbf{1b}$ ,  $\text{X} = \text{C}_6\text{F}_5$ ) with the Brønsted acid  $[\text{H}(\text{OEt}_2)_2]^+[\text{H}_2\text{N}\{\text{B}(\text{C}_6\text{F}_5)_3\}_2]^-$  ( $\text{HAB}_2$ ),<sup>17</sup> to create highly reactive  $[(\text{C}^{\wedge}\text{N}\text{-CH})\text{AuX}]^+$  cations. Here the anion does not compete for metal coordination sites, so that weak metal-ligand interactions can be observed.

The reactions of  $\mathbf{1a}$ ,  $\mathbf{b}$  with 1 equiv  $\text{HAB}_2$  in  $\text{CD}_2\text{Cl}_2$  afford the protodeauration products  $[(\text{C}^{\wedge}\text{N}\text{-CH})\text{AuX}(\text{OEt}_2)]^+\text{AB}_2^-$  ( $\mathbf{2a}$ ,  $\mathbf{b}$ ) in quantitative yields. Full NMR characterization supported the formulation as ion pairs with non-coordinating amido-diborate counterions. Diffusion NMR experiments demonstrated the monomeric nature of the cations and  $\text{Et}_2\text{O}$  coordination; the latter was further confirmed by the presence of selective dipolar interactions between  $\text{Et}_2\text{O}$  protons and aromatic resonances in the  $^1\text{H}$  NOESY NMR spectrum (see ESI,† Fig. S11–S13).

Rather unexpectedly, analysis of the dipolar contacts in the NOE spectra of  $\mathbf{2a}$  and  $\mathbf{2b}$  revealed a selective chemical exchange process between protons  $5'$  of the protodeaured aryl ring with protons  $5$  of the metal-bound phenyl (Scheme 2 and ESI,† Fig. S5 and S6). This observation suggests that protodeauration is reversible on the NOE timescale, due to the efficient C–H activation of the pendent aryl ring, which regenerates a transient concentration of  $\mathbf{1}$ , together with the release of the acid.

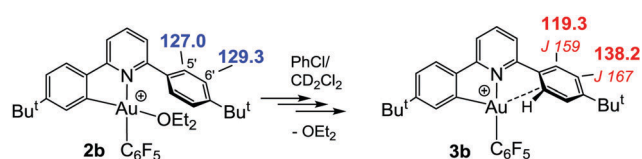
For  $\mathbf{2a}$  at 323 K the rate of exchange  $k_{\text{EX}}(\mathbf{2a})$  was  $2.3 \text{ s}^{-1}$ , leading to an exchange barrier of  $\Delta G^\ddagger = 18.3 \text{ kcal mol}^{-1}$  ( $^1\text{H}$  EXSY NMR,  $\text{C}_6\text{D}_5\text{Cl}$ ). An Eyring analysis over  $T = 298\text{--}343 \text{ K}$  allowed the determination of  $\Delta H^\ddagger = 11 \text{ kcal mol}^{-1}$  and a negative activation entropy,  $\Delta S^\ddagger = -23 \text{ cal mol}^{-1} \text{ K}^{-1}$ . The rate of exchange of the perfluorophenyl complex  $\mathbf{2b}$  was slightly slower,  $k_{\text{EX}}(\mathbf{2b}) = 1.1 \text{ s}^{-1}$  ( $\Delta G^\ddagger = 18.8 \text{ kcal mol}^{-1}$  at 323 K). Other cationic Au–aryl complexes such as  $\mathbf{1c}$  ( $\text{X} = p\text{-C}_6\text{H}_4\text{F}$ ) or  $\mathbf{1d}$  ( $\text{X} = \text{C}_6\text{H}_5$ ) gave analogous cleavage products  $\mathbf{2c}$ ,  $\mathbf{2d}$  but without any indication of reversibility on the NOE timescale, which suggests that in these cases cyclometallation is more difficult ( $\Delta\Delta G^\ddagger \geq 3.5 \text{ kcal mol}^{-1}$ , considering an NOE-observation limit of  $k_{\text{EX}} \approx 0.01 \text{ s}^{-1}$ ).



Scheme 2 Ether-mediated reversible Au–C protonation/C–H deprotonation, showing the atomic numbering used for NMR assignments.

Generating  $\mathbf{2b}$  in chlorobenzene- $d_5$  at room temperature followed by several vacuum/ $\text{CD}_2\text{Cl}_2$  cycles gives solutions which are essentially free of diethyl ether. The resulting changes in the NMR spectra, especially of the signals of the “dangling”  $\text{C}_6\text{H}_4\text{Bu}^t$  substituent, are consistent with the conversion of  $\mathbf{2b}$  to a new species  $\mathbf{3b}$ . Thus the unremarkable  $^{13}\text{C}$  NMR chemical shifts of the *o*- and *m*-C atoms in  $\mathbf{2b}$  ( $\text{C}5'$ ,  $\text{C}6'$ , respectively, Scheme 3) move from  $\delta_{\text{C}} = 127.0$  and  $129.3$  to  $\delta_{\text{C}} = 119.3$  ( $\text{C}5'$ ) and  $138.2$  ppm ( $\text{C}6'$ ) in  $\mathbf{3b}$ . On the other hand, there is no major change in  $^1J_{\text{C,H}}$  values ( $\mathbf{2b}$ :  $^1J_{\text{C,H}} = 160 \text{ Hz}$  for  $\text{C}5'$  and  $\text{C}6'$ ;  $\mathbf{3b}$ :  $^1J_{\text{C,H}} = 159$  ( $\text{C}5'$ ) and  $167 \text{ Hz}$  ( $\text{C}6'$ )).

The data are consistent with an interaction between the gold ion and the “dangling” aryl side-arm. The  $\text{C}^{\wedge}\text{N}\text{-CH}$  ligand system is too strained to allow  $\eta^2$ -type  $\pi$ -coordination of  $\text{C}_6\text{H}_4\text{Bu}^t$  to the metal centre. Steric factors also dictate that the only way the  $\text{C}_6\text{H}_4\text{Bu}^t$  moiety in  $\mathbf{3b}$  can approach the metal is by tilting by about  $45^\circ$  relative to the  $(\text{C}^{\wedge}\text{N})\text{Au}$  plane, to maximize the interaction of Au with one of the *ortho*-C atoms ( $\text{C}5'$ ). Since the bilateral symmetry of  $\text{C}_6\text{H}_4\text{Bu}^t$  is retained in the  $^1\text{H}$  NMR spectrum, there must be rapid interchange between the two *ortho* positions, which suggest that the Au...arene interaction is rather weak. Consistent with this, VT  $^1\text{H}$  NMR spectra down to  $-85^\circ\text{C}$  showed broadening of the  $\text{H}5'$  resonance but no loss of symmetry. Evidently the tilting motion is not frozen at that temperature, so that gold alternately interacts with both  $\text{C}5'$  atoms.‡ Thus the metal polarizes the aryl substituent, but without significant deformation of the aryl C–H bond which would result in changes in the  $^1J_{\text{C,H}}$  coupling constant. Such an interaction is most in line with the model proposed for a CMD intermediate (Scheme 1b). It appears therefore that with  $\mathbf{3b}$  it has been possible to generate such a species as a local minimum structure.



Scheme 3 Generation of ether-free gold cations indicating changes in the  $^{13}\text{C}$  NMR data of the aryl substituent ( $^1J_{\text{C,H}}$  values in italics).



Another instructive difference between the ether complex **2b** and ether-free **3b** concerns the proton shuttling process. Whereas in **2b** proton exchange leads to reversible C–H activation, as described above, ether-free complexes **3a**, **3b** show no H<sup>+</sup> mobility: protodeauration is no longer reversible. As has been amply demonstrated kinetically and in computational models, in palladium-mediated C–H activations by the CMD mechanism it is the bridging acetate that enables the deprotonation step.<sup>11–13</sup> The facile proton exchange in gold complexes of type **2** shows that this role can also be fulfilled by a weakly basic solvent: at least one ether molecule is required for proton shuttling. In its absence, Au–C cleavage becomes irreversible. To our knowledge this is the first clear illustration of the role of even weakly binding solvents in C–H activation processes in gold chemistry.

The observed proton shuttling, the role of solvent, and the proposed structure of a CMD-type arene complex were further supported by modelling studies using density functional theory (DFT) calculations. The mechanism of proton exchange in **2a**, the reaction pathway and its energy profile are shown in Scheme 4.

At the starting point, the oxidative protonation of an Au<sup>III</sup> complex to a cationic Au<sup>V</sup> intermediate was checked but quickly ruled out. We therefore focused on direct Au–C protonation. In order to explore mechanistic variations, we used a simplified model ligand lacking the *t*Bu substituents and H(OMe)<sub>2</sub><sup>+</sup> as a model for [H(OEt)<sub>2</sub>]<sub>2</sub><sup>+</sup>[H<sub>2</sub>N{B(C<sub>6</sub>F<sub>5</sub>)<sub>3</sub>]<sub>2</sub><sup>−</sup>, to minimise conformational issues. Structures were fully optimized in the presence of a solvent model (chlorobenzene, PCM model of Gaussian09).

It was assumed that the acid H(OR)<sub>2</sub><sup>+</sup> approaches the neutral complex **A** to give the association complex **C** *via* transition state **TS-B**. The formation of **TS-B** is associated with the negative entropy that was experimentally observed for the overall process, since the path from **C** to **F** is essentially entropy-neutral. In **C** the acidic

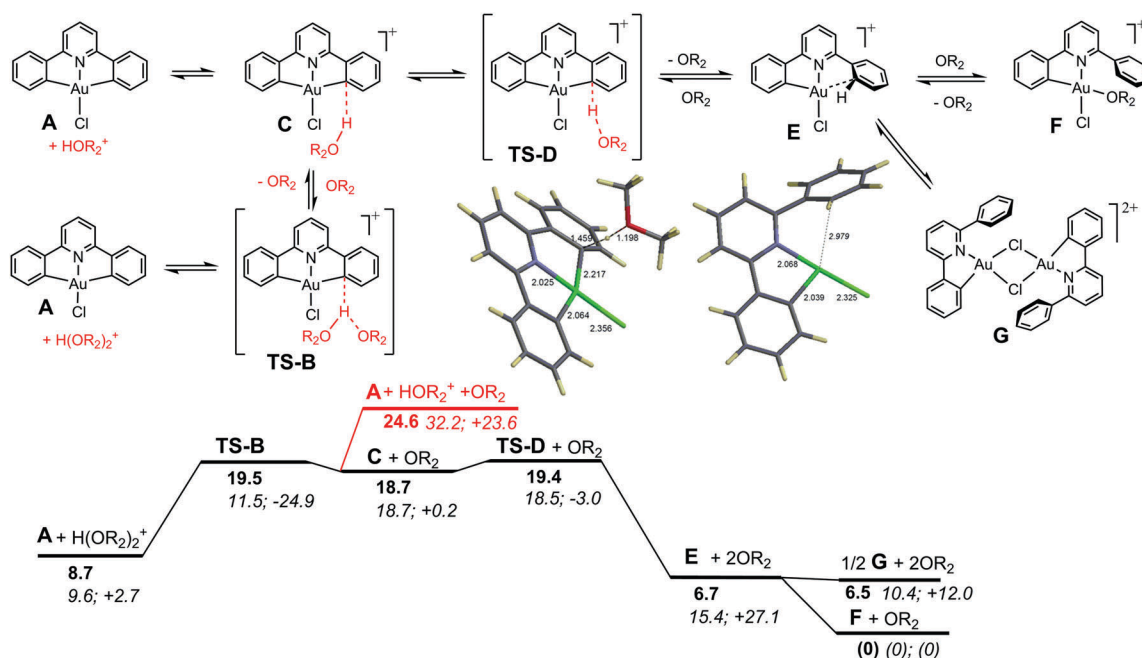
O–H bond has already approached the Au–C bond quite closely (H–O = 1.01 Å; H...C = 1.93 Å). From there, the proton is transferred to carbon with a very small barrier (≤1 kcal mol<sup>−1</sup>, *via* **TS-D**) to produce three-coordinate complex **E**, releasing the conjugate base OR<sub>2</sub>. This intermediate may then dimerize to **G**, although the energetically preferred pathway is to capture OR<sub>2</sub> to form the ether complex **F**.

Further checks showed that the use of OEt<sub>2</sub> instead of OMe<sub>2</sub> as a base reduces the exchange barrier by 3–4 kcal mol<sup>−1</sup>. About half of that (~2 kcal mol<sup>−1</sup>) is due to the lower complexation energy (presumably for steric reasons) of OEt<sub>2</sub> to Au; the remainder is likely related to the higher Brønsted basicity of OEt<sub>2</sub> compared to OMe<sub>2</sub>.

There is an equivalent pathway which assumes dissociation of H(OR)<sub>2</sub><sup>+</sup> into HOR<sub>2</sub><sup>+</sup> + OR<sub>2</sub> prior to attack on complex **A**. However, this would not explain the observed negative activation entropy.

The potential-energy surface is rather flat around the relevant species **C** + OR<sub>2</sub>, **TS-B** and **A** + H(OR)<sub>2</sub><sup>+</sup>, but a stationary point with the correct geometry and reaction coordinate for such a proton transfer could be located. In this scenario **TS-B** is (barely) rate-limiting. The calculated effective activation parameters for the simplified model system ( $\Delta H^\ddagger = 11.5$  kcal mol<sup>−1</sup>,  $\Delta S^\ddagger = -24.9$  cal mol<sup>−1</sup> K<sup>−1</sup>,  $\Delta G^\ddagger = 19.5$  kcal mol<sup>−1</sup> at 50 °C) agree well with the ones derived from the Eyring analysis for the real system. Over the stages **TS-D** ⇌ **C** ⇌ **TS-B** the free-energy profile is virtually flat (within 2 kcal mol<sup>−1</sup>), but the partitioning in  $\Delta H^\ddagger$  and  $T\Delta S^\ddagger$  varies considerably.

Alternatively, the acid complex **C** could rearrange to have the O–H bond interact with the second Au-bound carbon (a **TS** could not be located), which would lead to a presumably somewhat lower barrier of at least 19 kcal mol<sup>−1</sup> for the intramolecular proton exchange, in close agreement with the



**Scheme 4** Reversible deprotonation pathway for (C<sup>N</sup>C)AuCl with calculated stationary points for **TS-D** and species **E** (top) and calculated free-energy profile [bold:  $\Delta G$  (kcal mol<sup>−1</sup>); in italics:  $\Delta H$  (kcal mol<sup>−1</sup>);  $\Delta S$  (cal mol<sup>−1</sup> K<sup>−1</sup>)].



observation. On the other hand, intermolecular proton exchange would involve formation of **A** and free  $\text{HOR}_2^+$  as the highest-energy point of the reaction, with a calculated  $\Delta G(\text{F-A} + \text{HOR}_2^+)$  of  $\sim 25 \text{ kcal mol}^{-1}$ , which is somewhat higher than was observed experimentally.

The effect of substituents **X** on the proton exchange reaction was explored assuming that the path involving **TS-B** shown in Scheme 4 can be extended to variations of the Au complex, and that in all cases the variation in free energy over these structures is small. This allows us to use the free energy difference  $\Delta G^\ddagger(\text{F-TS-D})$  as a first estimate of the effective deprotonation barrier (see ESI,† Table S4 for a summary of the predicted substituent effects on deprotonation barriers).

For complexes bearing aryl groups at Au one could also envisage competing protonation of the non-chelated Au–aryl bond. The barrier calculated for this process (for  $\text{X} = \text{C}_6\text{H}_5$ ) is  $\sim 7 \text{ kcal mol}^{-1}$  higher than for protonation at the  $\text{C}^{\wedge}\text{N}^{\wedge}\text{C}$  ligand, in agreement with the observed selective protonation of the Au–C bond of the pincer ligand. Two factors that are important here are the ring strain in the  $(\text{C}^{\wedge}\text{N}^{\wedge}\text{C})\text{Au}$  framework (promoting ligand protonation) and the out-of-plane orientation of the aryl group at Au (hindering its protonation).

The possible structure of the ether-free complex **3b** was also interrogated by DFT methods. No evidence was found for agostic  $\text{Au}\cdots\text{H-C}$  bonding<sup>18</sup> or a  $\pi$ -complex. The optimized structure converges to a situation with rather long contacts with the metal, Au–*ortho*-C 2.81 Å and Au–H 2.61 Å and no evidence for a strong Au–(CH) interaction; the H atom is bent out of plane of the 6-ring by less than 10 degrees. Calculations of the <sup>13</sup>C NMR chemical shifts for ether-bound **2b** and solvent-free **3b** confirmed the observed chemical shift trends (with the simplification that  $\text{OMe}_2$  was used in the model). For **2b**, <sup>13</sup>C shifts in the range expected for a non-bound phenyl group were calculated,  $\delta$  129.47 and 128.23 for the C5' and C6' signals of  $-\text{C}_6\text{H}_4\text{Bu}^t$ , respectively. In the model of solvent-free **3b**, with the  $-\text{C}_6\text{H}_4\text{Bu}^t$  substituent tilted by 45° relative to the plane through the  $(\text{C}^{\wedge}\text{N})\text{Au}$  chelate, shifts of  $\delta$  117.5 and 130.7 (C5, C5'; average 124.1) and 133.29 and 135.76 (C6, C6'; average 134.5) were determined, which qualitatively reflect the observed increase in  $\Delta\delta$  between the *o*- and *m*-C chemical shifts. On rotation of the ring to 90° these differences disappear. According to Wiberg bond indices, in the naked  $[(\text{C}^{\wedge}\text{N-CH})\text{Au}]^+$  ion the interaction of Au with the nearby *ortho*-carbon atom amounts to about 10% of a full covalent Au–C bond (using the true Au–C bond as reference). This interaction reduces to about 1–2% on rotation of the phenyl ring to a perpendicular orientation, or on coordination of  $\text{OMe}_2$  to the empty site. The direct interaction of Au with the *ortho*-hydrogen is always very small. The calculations appear to slightly underestimate the metal–arene interaction compared to the experimental NMR data but are generally consistent with observation. The best model appears to be the type of incipient near-perpendicular metal–arene interactions envisaged in the CMD mechanism (Scheme 1b), whereas the data do not support the formation of a Wheland-type intermediate. In the active proton shuttling process such structures would be close to the transition state. In the absence of a solvent to provide  $\text{H}^+$  mobility, weak metal–arene bonding becomes a resting state.

In summary, we show here that (i) both Au–C bond cleavage and C–H activation in well-defined gold(III) systems can be both facile and reversible; (ii) proton shuttling depends on the presence of a weakly basic solvent, in this case ether, which facilitates proton abstraction from a metal-bound arene; (iii) in the absence of such a solvent, proton exchange is arrested and a structure with a polarized aryl through gold–arene  $\pi$ -interaction becomes the spectroscopically detectable ground state. Metal–arene interactions of this type have previously been proposed for C–H activation processes by the Concerted Metallation-Deprotonation (CMD) mechanism. To our knowledge, the present results provide the first experimental evidence for such interactions.

This work was supported by the European Research Council. M. B. is an ERC Advanced Investigator Award holder (grant no. 338944-GOCAT).

## Notes and references

† The aryl oscillation implies that the observed NMR parameters of C5' and C6' in **3b** are average values.

- (a) J. Le Bras and J. Muzart, *Chem. Rev.*, 2011, **111**, 1170; (b) M. Albrecht, *Chem. Rev.*, 2010, **110**, 576; (c) D. Alberico, M. E. Scott and M. Lautens, *Chem. Rev.*, 2007, **107**, 174; (d) T. Gensch, M. N. Hopkinson, F. Glorius and J. Wencel-Delord, *Chem. Soc. Rev.*, 2016, **45**, 2900; (e) Z. X. Huang, H. N. Lim, F. Y. Mo, M. C. Young and G. B. Dong, *Chem. Soc. Rev.*, 2015, **44**, 7764; (f) M. N. Hopkinson, A. D. Gee and V. Gouverneur, *Chem. – Eur. J.*, 2011, **17**, 8248.
- R. Kumar and C. Nevado, *Angew. Chem., Int. Ed.*, 2017, **56**, 2.
- D.-A. Roşca, J. A. Wright and M. Bochmann, *Dalton Trans.*, 2015, **44**, 20785.
- (a) V. W.-W. Yam, V. K.-M. Au and S. Y.-L. Leung, *Chem. Rev.*, 2015, **115**, 7589; (b) G. S. M. Tong, K. T. Chan, X. Y. Chang and C.-M. Che, *Chem. Sci.*, 2015, **6**, 3026; (c) A. Szentkuti, M. Bachmann, J. A. Garg, O. Blacque and K. Venkatesan, *Chem. – Eur. J.*, 2014, **20**, 2585.
- (a) J. Fernandez-Cestau, B. Bertrand, M. Blaya, G. A. Jones, T. J. Penfold and M. Bochmann, *Chem. Commun.*, 2015, **51**, 16629; (b) L. Currie, J. Fernandez-Cestau, L. Rocchigiani, B. Bertrand, S. J. Lancaster, D. L. Hughes, H. Duckworth, S. T. E. Jones, D. Credgington, T. J. Penfold and M. Bochmann, *Chem. – Eur. J.*, 2017, **23**, 105.
- (a) B. Bertrand and A. Casini, *Dalton Trans.*, 2014, **43**, 4209; (b) T. T. Zou, C. T. Lum, C.-N. Lok, J.-J. Zhang and C.-M. Che, *Chem. Soc. Rev.*, 2015, **44**, 8786.
- (a) M. S. Kharasch and H. S. Isbell, *J. Am. Chem. Soc.*, 1931, **53**, 3053; (b) Y. Fuchita, Y. Utsunomiya and M. Yasutake, *J. Chem. Soc., Dalton Trans.*, 2001, 2330.
- Y. Liu, Z. Z. Yu, J. Z. H. Zhang, L. Liu, F. Xia and J. L. Zhang, *Chem. Sci.*, 2016, **7**, 1988.
- (a) P. F. Lu, T. C. Boorman, A. M. Z. Slawin and I. Larrosa, *J. Am. Chem. Soc.*, 2010, **132**, 5580; (b) I. I. F. Boogaerts and S. P. Nolan, *Chem. Commun.*, 2011, **47**, 3021, and cited references.
- D.-A. Roşca, D. A. Smith and M. Bochmann, *Chem. Commun.*, 2012, **48**, 7247.
- D. Garcia-Cuadrado, P. de Mendoza, A. A. C. Braga, F. Maseras and A. M. Echavarren, *J. Am. Chem. Soc.*, 2007, **129**, 6880.
- L. Ackermann, *Chem. Rev.*, 2011, **111**, 1315.
- S. I. Gorelsky, D. Lapointe and K. Fagnou, *J. Org. Chem.*, 2012, **77**, 658.
- M. K. Ghosh, M. Tilset, A. Venugopal, R. H. Heyn and O. Swang, *J. Phys. Chem. A*, 2010, **114**, 8135.
- (a) L. T. Ball, G. C. Lloyd-Jones and C. A. Russell, *Science*, 2012, **337**, 1644; (b) T. J. A. Corrie, L. T. Ball, C. A. Russell and G. C. Lloyd-Jones, *J. Am. Chem. Soc.*, 2017, **139**, 245.
- D. A. Smith, D.-A. Roşca and M. Bochmann, *Organometallics*, 2012, **31**, 5998.
- S. J. Lancaster, A. Rodriguez, A. Lara-Sanchez, M. D. Hannant, D. A. Walker, D. L. Hughes and M. Bochmann, *Organometallics*, 2002, **21**, 451.
- H. Schmidbaur, H. G. Raubenheimer and L. Dobrzańska, *Chem. Soc. Rev.*, 2014, **43**, 345.

